Ultrabroadband optical circular polarizers consisting of double-helical nanowire structures

Z. Y. Yang,[1,*] M. Zhao,[1] P. X. Lu,[1] and Y. F. Lu[2]

[1]*Wuhan National Laboratory for Optoelectronics, Huazhong University of Science and Technology, Wuhan, Hubei, 430074, China*

[2]*Department of Electrical Engineering, University of Nebraska-Lincoln, Lincoln, Nebraska, 68588-0511, USA*

**Corresponding author: zyang@mail.hust.edu.cn*

Received June 3, 2010; revised July 3, 2010; accepted July 5, 2010;
posted July 13, 2010 (Doc. ID 129500); published July 26, 2010

Recently, it was demonstrated by Gansel *et al.* [Science **325**, 1513 (2009)] that 3D single-helical metamaterials can serve as broadband circular polarizers in the IR range. In this study, we propose a structured metamaterial with double-helical nanowires to construct circular polarizers with boarder wavelength bands in the visible-light and near-IR regions. Using the finite-difference time-domain method, we confirmed that the circular polarizers with the double-helical structures have operation bands more than 50% broader than those of the single-helical structures.

OCIS codes: 260.5430, 160.3918, 160.1585.

Circular polarization of light is attractive for applications in reflective color displays [1–3], microscopy in life science, and photography [4,5]. Generally, there are two ways of obtaining circular polarized light. One is the use of a linear polarizer and a quarter-wave plate [6], which is the most common method in optical engineering; the other is utilizing cholesteric liquid crystals (CLCs) [7–10], which are self-assembled photonic crystals formed by rodlike molecules. However, both approaches are restricted to narrow frequency ranges, which is a major limitation in many applications [11].

Recently, Gansel *et al.* [11,12] succeeded in developing broadband circular polarizers using metamaterials consisting of single-helical gold nanowires. The devices offer giant circular dichroism in a wavelength region of 3–6 μm. Compared with the former two methods, the helical circular polarizers have advantages of broad operation bands and compact structures that can be conveniently integrated with other optical devices.

In this Letter, we propose a type of circular polarizers with double-helical nanowire metamaterials, for the purpose of further increasing the operation bands. The optical properties of the proposed circular polarizers were studied to compare with those of the single-helical ones by the finite-difference time-domain (FDTD) method. From the simulation results, we found that the polarizers with the double-helical nanowire metamaterials have operation bands more than 50% broader than the single-helical structures. This phenomenon of ultrabroadband polarization can be explained qualitatively through an effective model of the helical circular polarizers. It is expected that the circular polarizers with double-helical structures can be tuned to operate in various wavelength regions by scaling the structure size, as long as the operation wavelength is well below the metal plasma frequency.

Circular polarizers consisting of metamaterials with single- and double-helical nanowires were simulated using the FDTD method. Figure 1 shows the schematic diagram of a polarizer with the double-helical nanowire structure, in which DW, NH, SG, LH, and DH stand for the diameter of the wire, the number of the helix periods, the spacing of the grid, the length of the helix period, and the diameter of the helix, respectively. The parameters of the metamaterial structure are DW = 50 nm, NH = 3, SG = 190 nm, LH = 200 nm, and DH = 100 nm. The helical nanowire structure is supported by a silica substrate. We assume that the refractive index of silica is 1.45, independent of the frequency in the visible and near-IR ranges. Two circularly polarized states of light, left-handed circular polarization (LCP) and right-handed circular polarization (RCP), were used as the excitation sources to irradiate the polarizers along the positive Z direction, respectively. To simplify the simulation, a broadband Gaussian-modulated pulsed light source is used as the excitation source, which can be expressed as

$$T(t) = \exp\left[-\frac{1}{2}\left(\frac{t - t_{\text{off}}}{t_w}\right)^2\right]\sin(\omega t), \tag{1}$$

where t_{off} is the offset time, t_w is the half width of the pulse, and ω is the central frequency of the source. The perfectly matched layers (PMLs) [13] were along the Z direction. The boundaries along X and Y directions were

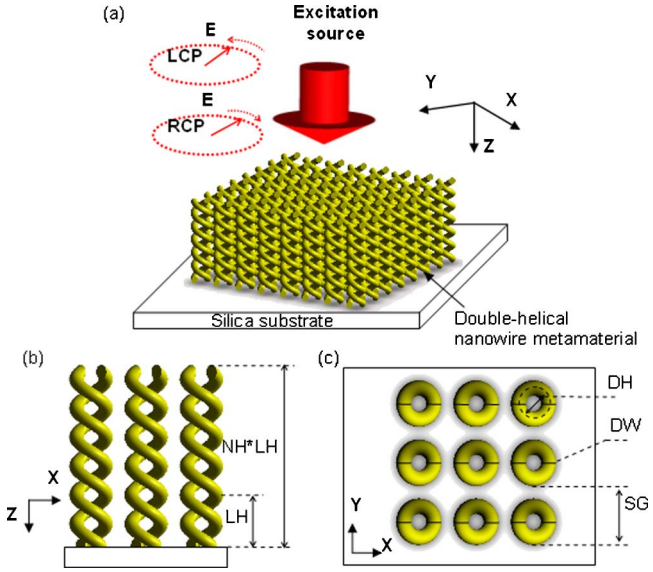

Fig. 1. (Color online) Schematic diagram of the optical circular polarizer used in numerical simulations.

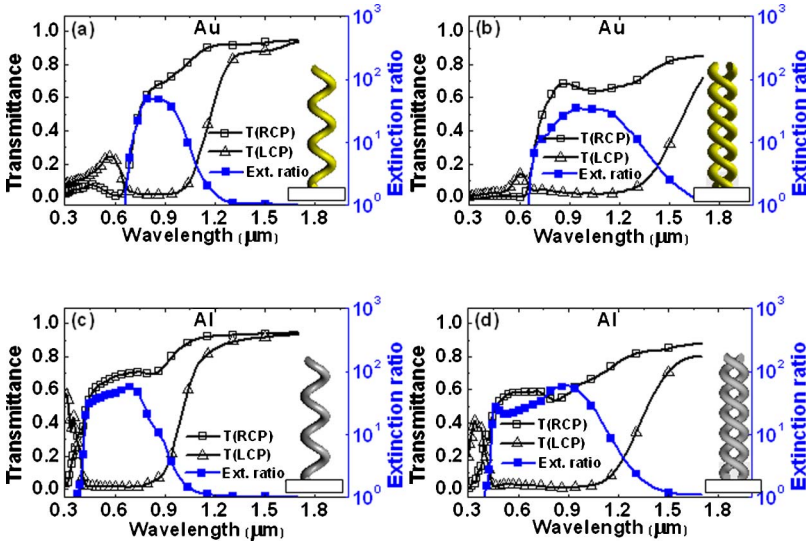

Fig. 2. (Color online) Comparison of the optical performances between single- and double-helical nanowire metamaterials: (a), (b) Au single- and double-helix; (c), (d) Al single- and double-helix.

confined with the periodic boundary conditions [14] owing to the periodicity of the nanowire metamaterials.

During the calculation, the dielectric functions of the metal materials were described by the Lorentz–Drude model, which can be expressed as [15]

$$\varepsilon_r(\omega) = \left[1 - \frac{\Omega^2}{\omega(\omega - i\Gamma_0)}\right] + \left[\sum_{j=1}^{k} \frac{f_j \omega_p^2}{(\omega_j^2 - \omega^2) + i\omega\Gamma_j}\right], \quad (2)$$

where ω_p is the plasma frequency; k is the number of oscillators with frequency ω_j, strength f_j, and lifetime $1/\Gamma_j$; while $\Omega = \sqrt{f_0} \cdot \omega_p$ is the plasma frequency associated with intraband transitions with oscillator strength f_0 and damping constant Γ_0.

Circular polarizers with either the single- or double-helical nanowire structures with two different metals, gold (Au) and aluminium (Al), were simulated using the FDTD method. Their optical performances are shown in Fig. 2. Figures 2(a) and 2(c) are transmittances of the circular polarizers for the LCP and RCP light beams and the extinction ratio as functions of the wavelength for the single-helical structure of Au and Al nanowires, respectively. Figures 2(b) and 2(d) are the results for the double-helical structure of Au and Al nanowires, respectively.

The operation regions of the circular polarizers are defined as the wavelength regions in which the extinction ratio is not less than $1/e$ of its peak value. From the simulation results, the average transmittances for the RCP light and the average extinction ratios in the operation regions are shown in Fig. 2 and listed in Table 1. It is very clear that the operation regions of the circular polarizers with the double-helical structures are more than 50% broader than those of the single-helical structures. The operation regions of the circular polarizers can be tuned into different wavelength ranges by scaling the structure sizes, as long as the operation wavelength is sufficiently below the metal plasma frequency [11].

Table 1. Comparison of the Optical Performances between Single- and Double-Helical Nanowire Metamaterials

	Operation Regions [μm]	Average Transmittances of RCP Light	Average Extinction Ratios
Au Single-helix	0.72–1.00	63%	36:1
Double-helix	0.75–1.30	65%	25:1
Al Single-helix	0.42—0.79	63%	39:1
Double-helix	0.44–1.10	56%	31:1

Figures 3(a) and 3(b) are single-frame excerpts from video clips simulating the RCP and LCP light propagating through a circular polarizer consisting of double-helical Al nanowires, respectively. The RCP light transmits through the polarizer, but the LCP light does not.

Our simulation model is based on the helical antennas with the so-called end-fire geometry. Such helical antennas are widely used in microwave wireless local-area network (WLAN) applications [16]. In antenna theory, the same handedness of electromagnetic wave interacts with the helical structure antennas. In contrast, the opposite handedness of electromagnetic wave is not expected to interact with the antennas. Thus, the helical metamaterial structure exhibits giant circular dichroism.

The structures of the circular polarizers can be regarded as two parts: one is the F–P cavity, and the other is the helical metamaterial. The optical performances of the circular polarizers, such as the operation bands, depend on both characteristics of these two parts. As we

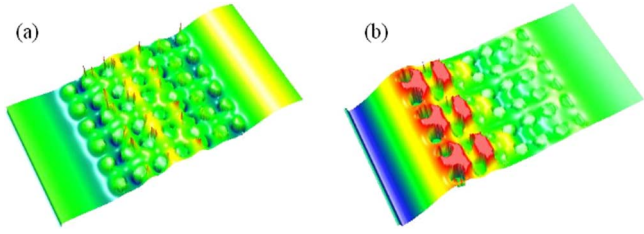

Fig. 3. (Color online) Single-frame excerpts from video clips simulating the RCP and LCP light propagation through the Al circular polarizer: (a) RCP light (Media 1), (b) LCP light (Media 2).

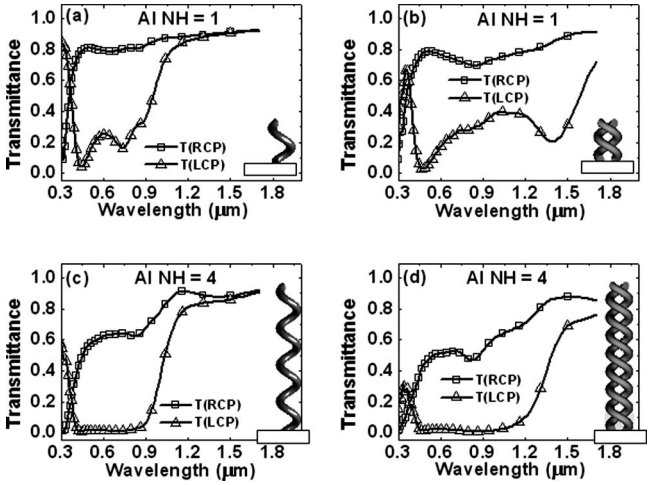

Fig. 4. Optical performances of circular polarizers with different numbers of helix period.

know, the transmittance of the F–P cavity has a multivalley spectrum. The transmittance curve of the ideal helical structure has a circular polarization gap in a certain wavelength region [17]. For the overall performance of a circular polarizer, the dominant effect depends on the number of the helix period (NH). To verify our expectation, circular polarizers consisting of Al single- and double-helical metamaterials with different NHs were simulated, with results shown in Fig. 4. It is obvious that when NH = 1, the LCP transmittance spectrum of the circular polarizer exhibits two wave valleys, which indicates that the F–P cavity effect is dominant. When NH = 4, the LCP transmittance is almost zero in a certain wavelength region, which indicates that the helical structure effect is dominant. In addition, Fig. 4 also proves the advantage of the double-helical metamaterials to have broader operation bands. Compared with the single-helix structure, the double-helical structure has a larger average refractive index, which leads to the broadened space between two valleys of the F–P cavity, and the increased central wavelength of the polarization gap of the helical structure. Combining these two effects, the double-helical circular polarizers exhibit much broader operation bands than the single-helix ones.

In summary, optical circular polarizers with double-helical nanowire metamaterials were studied. It was found that the double-helical circular polarizers have much broader operation bands than the single-helical ones. The theories governing the F–P cavity and the helical structures were successfully used to explain the reasons of realizing the ultrabroadband operation. However, there are some other factors that lead to broadening of the operation bandwidth, e.g., the interactions between the two helix wires in a double-helical wire, which does not exhibit in the present model. Thus, to develop another more precise physical model is one of our next works. Although the proposed structures need to be fabricated to experimentally realize the circular polarizers, the ultrabroadband circular polarizers will provide a new type of component in advanced optical applications.

This work was supported by the National Natural Science Foundation of China (NSFC) (Nos. 10874024 and 50735007), the Doctoral Fund of Ministry of Education of China (No. 200804871147), the Natural Science Foundation of Hubei Province of China (No. 2008CDB004), and also partly supported by the China National Funds for Distinguished Young Scientists (No. 66945021) and the "973" program of China (No. 2010CB923203).

References

1. J. Lub, P. van de Witte, C. Doornkamp, J. P. A. Vogels, and R. T. Wegh, Adv. Mater. **15**, 1420 (2003).
2. G. De Filpo, F. P. Nicoletta, and G. Chidichimo, Adv. Mater. **17**, 1150 (2005).
3. T. Yoshioka, T. Ogata, T. Nonaka, M. Moritsugu, S. N. Kim, and S. Kurihara, Adv. Mater. **17**, 1226 (2005).
4. A. Lokształjn and W. Dzwolak, J. Mol. Biol. **395**, 643 (2010).
5. K. Claborn, E. Puklin-Faucher, M. Kurimoto, W. Kaminsky, and B. Kahr, J. Am. Chem. Soc. **125**, 14825 (2003).
6. E. Hecht, *Optics*, 4th ed. (Addison-Wesley, 2002).
7. R. A. M. Hikmet and H. Kemperman, Nature **392**, 476 (1998).
8. M. Mitov and N. Dessaud, Nat. Mater. **5**, 361 (2006).
9. J. M. Xiao, H. Cao, W. L. He, Z. Ma, J. Geng, L. P. Wang, G. Wang, and H. A. Yang, J. Appl. Polym. Sci. **105**, 2973 (2007).
10. N. Y. Ha, Y. Ohtsuka, S. M. Jeong, S. Nishimura, G. Suzaki, Y. Takanishi, K. Ishikawa, and H. Takezoe, Nat. Mater. **7**, 43 (2008).
11. J. K. Gansel, M. Thiel, M. S. Rill, M. Decker, K. Bade, V. Saile, G. von Freymann, S. Linden, and M. Wegener, Science **325**, 1513 (2009).
12. J. K. Gansel, M. Wegener, S. Burger, and S. Linden, Opt. Express **18**, 1059 (2010).
13. J. P. Berenger, J. Comput. Phys. **114**, 185 (1994).
14. P. Harms, R. Mittra, and W. Ko, IEEE Trans. Antennas Propagat. **42**, 1317 (1994).
15. A. D. Rakic, A. B. Djurisic, J. M. Elazar, and M. L. Majewski, Appl. Opt. **37**, 5271 (1998).
16. J. D. Kraus and R. J. Marhefka, *Antennas: for All Applications*, 3rd ed. (McGraw-Hill, 2003).
17. I. Abdulhalim, Appl. Opt. **47**, 3002 (2008).